remote sensing

MDPI

Article

Analysis of Daytime and Night-Time Aerosol Optical Depth from Solar and Lunar Photometry in Valladolid (Spain)

Celia Herrero del Barrio *, David Mateos, Roberto Román, Ramiro González, Sara Herrero-Anta, Daniel González-Fernández, Abel Calle, Carlos Toledano, Victoria Eugenia Cachorro and Ángel Máximo De Frutos Baraja

Group of Atmospheric Optics (GOA), University of Valladolid, 47011 Valladolid, Spain; mateos@goa.uva.es (D.M.); robertor@goa.uva.es (R.R.); ramiro@goa.uva.es (R.G.); sara@goa.uva.es (S.H.-A.); daniel@goa.uva.es (D.G.-F.); abel@goa.uva.es (A.C.); toledano@goa.uva.es (C.T.); chiqui@goa.uva.es (V.E.C.); angel@goa.uva.es (Á.M.D.F.B.)

* Correspondence: celia@goa.uva.es

Abstract: Aerosol optical depth (AOD) at night-time has become a hot topic in recent years due to the development of new instruments recording accurate ground-based lunar irradiance measurements, and the development of calibration methods and extraterrestrial irradiance models adapted to lunar photometry. This study uses all daytime and night-time AOD data available at Valladolid (Spain) from October 2016 to March 2022 in order to analyze its behavior and the added contribution of night data. The annual, monthly and daily AOD evolution is studied comparing daytime and night-time values and checking the correlation between them. For this purpose, the daily averages are computed, showing an annual pattern, with low AOD values throughout the year (mean value of AOD at 440 nm: 0.122), where winter months have the lower and summer the higher values, as observed in previous studies. All these AOD values are modulated by frequent desert dust events over the Iberian Peninsula, with a strong influence on daily and monthly mean values in February and March, where the strongest desert outbreaks occurred. The added new data confirm these results and the good correlation between daytime and night-time data. Also, a complete daily evolution is shown, observing that AOD and Ångström exponent (AE) mean values vary by only ±0.02 in 24 h, with a maximum value at 06:00 UTC and minimum at 18:00 UTC for both parameters.

Keywords: lunar photometry; aerosol optical depth; Ångström exponent; aerosol climatology; CAELIS

Citation: Herrero del Barrio, C.; Mateos, D.; Román, R.; González, R.; Herrero-Anta, S.; González-Fernández, D.; Calle, A.; Toledano, C.; Cachorro, V.E.; De Frutos Baraja, Á.M. Analysis of Daytime and Night-Time Aerosol Optical Depth from Solar and Lunar Photometry in Valladolid (Spain). *Remote Sens.* **2023**, *15*, 5362. https://doi.org/10.3390/rs15225362

Academic Editors: Tianning Su, Changqing Lin, Pengguo Zhao and Jing Wei

Received: 22 September 2023
Revised: 31 October 2023
Accepted: 9 November 2023
Published: 15 November 2023

1. Introduction

Atmospheric aerosols, which are particles floating in the atmosphere, interact directly with sunlight by scattering or absorption (aerosol-radiation interaction), but also, they act as condensation nuclei, which is known as aerosol–cloud interaction [1]. Both interactions have an impact on climate which, as they have an important role in radiative forcing, which is the difference between the radiation absorbed by Earth and the energy irradiated back to space [2]. The contribution of atmospheric aerosols to radiative forcing still remains uncertain [3], which highlights the need to measure and monitor the aerosol properties continuously on a global scale.

One of the most important aerosol optical properties in aerosol radiative forcing is the aerosol optical depth (AOD), which represents the light extinction by the aerosol following the Beer–Bouguer–Lambert law. AOD depends on wavelength, and this dependence is usually modelled in the solar range by the two parameters of Ångström's law [4,5]: Ångström exponent (AE), which provides information about AOD spectral dependence and aerosol size (lower AE, coarser particles); and turbidity parameter, which is the AOD at 1 µm wavelength.

There are several networks focused on monitoring AOD around the world, such as AERONET [6], GAW-PFR [7] and SKYNET [8]. AERONET (AErosol RObotic NETwork),

managed by NASA, is a federated network with over 500 measurement sites distributed worldwide. The standard instrument of AERONET is the Cimel CE318 radiometer (Cimel Electronique, Paris, France). Filter radiometers are generally used to derive spectral AOD and AE values measuring the direct solar irradiance at several wavelengths. The use of solar irradiance means that AOD can be obtained only during the daytime, which implies a lack of AOD data during the night-time and could lead to a bias in AOD climatology. In particular, this bias is more relevant in polar regions, where the sun is not visible for several months, i.e., the polar night. This led to long periods without data at high-latitude sites and a large uncertainty during the night when studying daily cycles.

To derive AOD at night-time periods, a new CE318 model (sun–sky–lunar CE318-T photometer) was developed by Cimel to measure solar but also lunar direct irradiances between first and third moon quarters, as the uncertainties increase under low moon illumination conditions [9]. This instrument allows the AOD calculation at night-time [9,10]. To calculate AOD from these ground-based direct lunar irradiance measurements, the extraterrestrial lunar irradiance (at the top of the atmosphere) is required. The extraterrestrial lunar irradiance is the sunlight reflected by the moon, and because of that, it varies significantly depending on different parameters such as the moon's albedo, moon's phase angle, moon–sun distance, and moon–Earth distance, among others. The ROLO model [11], or its freely available implementation RIMO [12], are generally used to estimate the extraterrestrial lunar irradiance (e.g., [13]). Román et al. [14] found that RIMO overestimates the extraterrestrial lunar irradiance and proposed a correction to RIMO to be used to derive AOD values from sun–moon photometers. The AOD values calculated using these corrected RIMO values and CE318-T photometer measurements, transferring solar calibration to lunar [9], are available at CAELIS (www.caelis.uva.es accessed on 8 November 2023; [15,16]).

Both networks mentioned previously, GAW-PFR and SKYNET, have also developed new implementations for their instruments in order to be able to measure AOD at night-time. In the case of the lunar PFR, the enhancing of the sensitivity for the standard instrument makes it possible to measure at four wavelengths (412, 500, 675 and 862 nm) with good continuity results in night-time measurements [17]. Regarding SKYNET reference instrument, POM-01 and POM-02 (Prede Ltd., Japan), it was modified in order to be able to measure low levels of irradiance by setting and amplifier and adjusting the tracker to follow the moon position at night. SKYNET uses the correction of the ROLO model proposed by Uchiyama et al. (2019) [18]; the results obtained for AOD presumably have the same degree of precision and accuracy within the measurement uncertainty for daytime and night-time [18].

In this framework, the main objective of this work is to obtain and analyze the seasonal cycle of daytime and night-time AOD and AE registered by solar and lunar photometry using measurements from a Cimel CE318 instrument, and computed with the CAELIS algorithm, for six years in a mid-sized urban station in north–central Spain. This study is also focused on the quantification of the 24-h cycle of AOD and AE, analyzing possible differences and similarities between the daytime and night-time cycles.

This paper is structured as follows: Section 2 presents the site, the data used, and the methodology followed. The main results and their discussion are presented in Section 3; while Section 4 summarizes the main conclusions of the work.

2. Site, Data and Method

The data of this work were recorded at the Valladolid AERONET station (4°39′49″N, 4°42′21″W, 705 m a.s.l.), located in the rooftop of the Science Faculty of Valladolid University. Valladolid is a medium-sized city with a population of 400,000 inhabitants, including its metropolitan area. It is located in the north–central part of the Iberian Peninsula, in the northern plateau of Spain (Castilian Plateau), which is surrounded by mountains, with continental aerosols being the most common aerosol type [19].

The Valladolid AERONET station is managed by the Group of Atmospheric Optics of the University of Valladolid (GOA-UVa). The GOA-Uva is involved in the calibration

tasks of AERONET instruments, and since 2019 has also been part of ACTRIS research infrastructure (Aerosols, Clouds, and Trace gases Research InfraStructure; www.actris.eu accessed on 8 November 2023). The AERONET photometers under calibration at Valladolid are calibrated through comparison against a master photometer previously calibrated at Atmospheric Observatory of Izaña (Tenerife, Spain) with the Langley method [20]; as a result, several sun–sky–lunar CE318-T photometers are always measuring side-by-side at Valladolid's station. Moreover, within the metrology project MAPP (www.pmodwrc.ch/en/mapp/, accessed on 10 October 2023), careful characterization of the Lunar photometers and calibration procedures have been carried out and implemented for this instrument. The dataset used in this study at Valladolid is formed by the records of three different CE318-T masters (#904, #942 and #949). This selection means that the period covered by the dataset at Valladolid is from October 2016 to March 2022, with a gap between March and June 2017, when there was not a lunar photometer in the site. No night-time data from master instruments were available prior to 2016.

The daytime and night-time AOD data from these photometers in the 2016–2022 period have been processed and obtained directly from CAELIS [15,16]. AOD at 340 nm has been not used since the low signal of lunar irradiance at this wavelength makes the AOD too noisy at night-time [14]. The AE has been calculated by a linear fit in log–log scale using the AOD values at 440, 500, 675 and 870 nm wavelengths. The AOD data have been previously cloud-screened following the method explained by González et al. [16], a cloud-screening method similar to the one proposed by Giles et al. [21]. The AOD sampling frequency for the CE318-T instruments is defined by AERONET protocols, and has increased over the years. Measurements at Valladolid were taken every 15 min until 2017, but since then the sampling period has been reduced to every 5 min during the day and every 3 min over the night.

All the AOD and AE data have been hourly, daily and monthly averaged separately. Hourly AOD and AE values have been obtained by averaging all the available data for every hour of the day for the whole period; these hourly data are useful to study the 24 h evolution of AOD and AE. The daily averages of AOD and AE have been calculated for each wavelength, differentiating between daytime and night-time, using all measurements within a day. The monthly mean (M), median (Md), standard deviation (sd), first (Q1) and third (Q3) quartile, and 5th (P5) and 95th (P95) percentiles of the hourly and daily datasets have been also calculated. These statistical estimators are useful to climatologically quantify the distribution of AE and AOD values [14–16,20,21].

3. Results and Discussion

3.1. Time Series of Aerosol Optical Depth and Ångström Exponent

The time series of monthly averages, derived from the available daily AE and AOD at 440 nm (AOD_{440}) values, is shown in Figure 1 for Valladolid. Both daytime and night-time averages are represented. The AOD and AE evolutions have a large variability at the monthly scale. Daytime and night-time values present a similar temporal evolution for both AOD_{440} and AE, although some differences can be seen, e.g., in February 2017 or March 2022. These differences could be explained, at least in part, by the fact that both daytime and night-time datasets cover different periods due to the variability of the presence of clouds and mainly due to the fact that lunar irradiance is only measured for half of each month (from the first to the third Moon quarter).

Generally, the lowest AOD_{440} values occurred during the winter months of December and January, while the larger ones usually happened in summer, some spring months and February. The standard deviation for night-time values seems larger than for daytime values in some months. Regarding AE, summer always presents mean values above 1, while the lowest values can be observed in general at winter and spring. The smaller AE values are associated with larger standard deviation values.

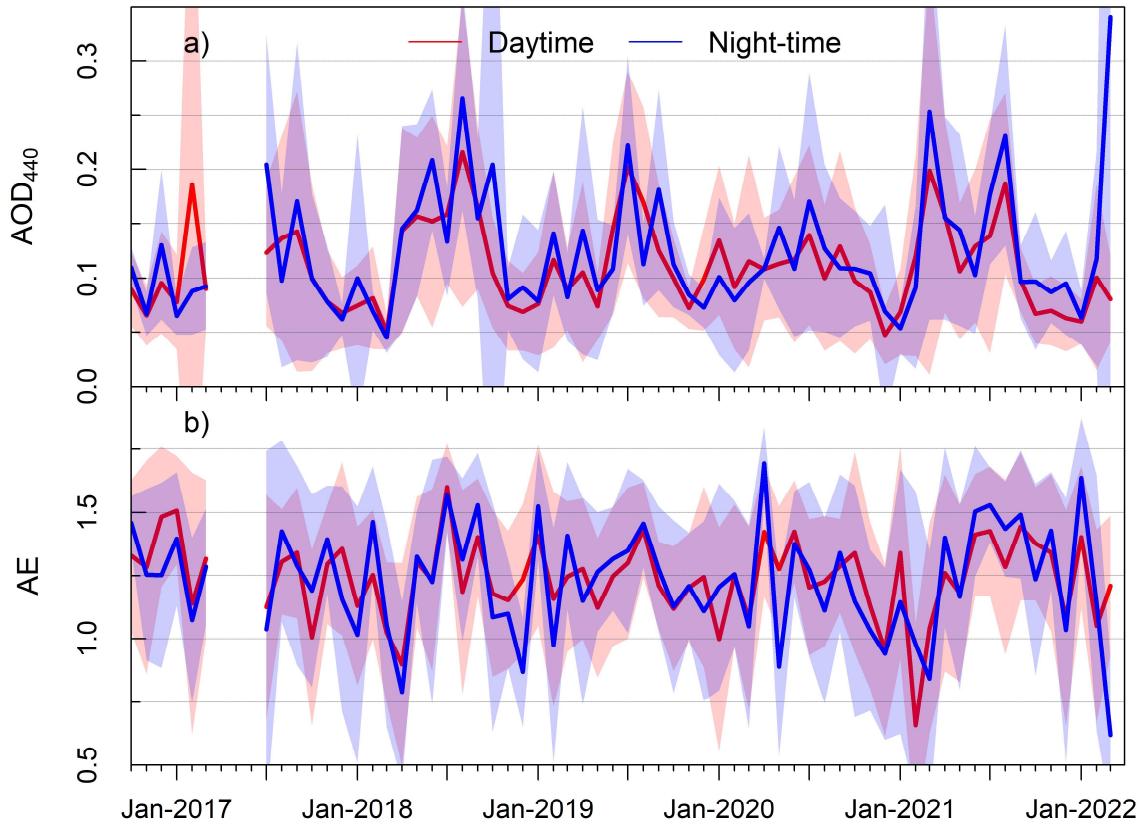

Figure 1. Time series of daytime and night-time monthly averages (derived from daily values) of aerosol optical depth at 440 nm (AOD_{440}; panel (**a**)) and Ångström exponent from 440 to 870 nm (AE; panel (**b**)) in Valladolid. The red and blue solid lines represent the monthly mean values, and the shaded band is the ± monthly standard deviation centered on the mean value. Red color is used for daytime measurements and blue for night-time.

The maximum AOD values associated with low AE values, and are caused by the presence of large particles like desert dust aerosols. These Saharan dust transport events happen at the Iberian Peninsula more often during summer [22], but the most intense events are seen in February and March [23]. Then, there are dust outbreaks for the whole year with large AOD values which present a variability of low AE values [24]; the observed results could indicate that desert dust events in summer reach Valladolid with AE values higher than in winter and spring, when the dust outbreaks are stronger. When high AOD values appear to be associated with high AE values, they are usually caused by the presence of smoke from bushfires, which also are more frequent in summer [25]. These bushfire events could be behind the higher AE values observed in summer. This indicates that different aerosol types govern aerosol seasonal distribution over Valladolid and the whole region. Regarding the year-to-year variability, the data from Valladolid do not show any significant trend. However, it would be necessary to analyze a longer period of time with more recorded data to obtain statistically significant results.

The evolution of the daily means can be seen in Figure A1 in the Appendix A, and corroborates the results presented here. Despite considering only 5 years, from October 2016 to March 2022, it is possible to see the large amount of data available, as well as showing the convenience of adding night-time measurements.

3.2. Annual Cycle

The statistical estimators (M, Md, sd, Q1, Q3, P5 and P95) of the monthly distributions of the daily AOD_{440} and AE values, during the daytime and night-time, are shown in

Figure 2. These estimators have been calculated using all the daily data available for each month of the data series.

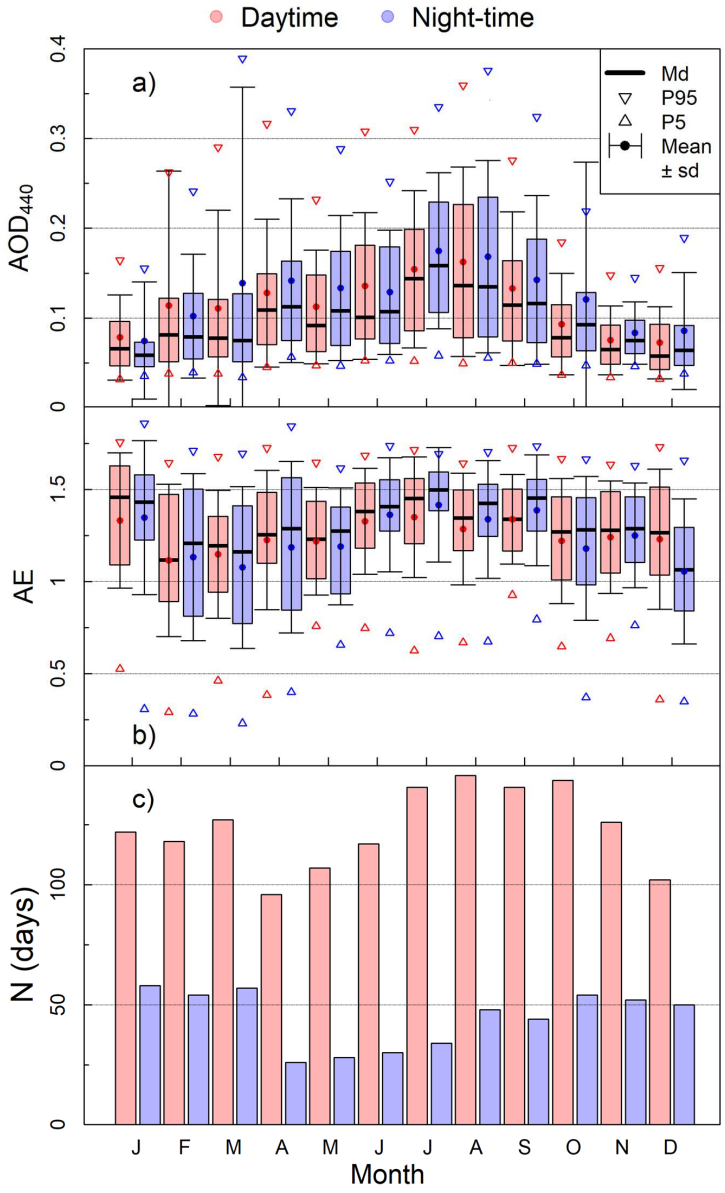

Figure 2. Box plot for the monthly evolution of aerosol optical depth at 440 nm (AOD_{440}; panel (**a**)) and Ångström exponent from 440 to 870 nm (AE; panel (**b**)) at Valladolid. The first (Q1) and third (Q3) quartile for the monthly dataset correspond to the upper and lower box limits. The median (Md) is represented by a horizontal black line, while the mean (M) is represented by a circle. The triangles show the 5th (P5) and 95th (P95) percentile values. The ± standard deviation is represented by an error bar centered on the mean value. The number of observations (N total days in each month for the whole time series) is shown in a histogram (panel (**c**)). Red values mean daytime, while blue is for night-time.

Regarding the values of AOD_{440} in Figure 2a, there are no significant differences in the monthly median between daytime and night-time datasets. In general, the median values for daytime are smaller than at night-time, as was observed in Lecce (Italy) by Perrone et al. [26], except in summer. In our case, this small displacement could be caused by having a smaller dataset at night that could have been contaminated by some outliers that were not detected by the cloud-screening. In fact, the shape of the seasonal cycle follows a similar

pattern for both daytime and night-time databases: the AOD_{440} increases progressively from winter to summer, July being the month with the highest median value for the AOD_{440} (0.16 during the night-time); then, after July, these AOD median values decrease to lower values until the end of the year, the median AOD_{440} value being around 0.06 for daytime measurements in December.

The mean values in the same figure seem less stable between day and night. The mean is not as robust as the median (it can easily become biased by few high values). In our dataset, monthly means are higher than median values for all months. This could be caused by the occurrence of high values during high aerosol load events, the maximum monthly values for AOD_{440} being 0.16 during the daytime in August, and 0.18 at night-time during July. The minimum values of the mean of AOD_{440} are 0.08 and 0.07 for daytime and night-time, respectively, both in January.

When comparing the daytime annual cycle obtained with the longer period available with AERONET direct sun AOD data in previous studies (e.g., [19,22]), which cover different time periods, some of the main features remain: AOD values increase during the first months of the year and present a local minimum value in May, with an increase again during summer months and a decrease in autumn. Figure A2 in Appendix A shows the monthly means for the whole time series in order to compare them with previous studies. However, in the last six years analyzed in this work, AOD values seem higher in summer than in the previous studies, with more than 10 years of data. In this sense, a reported local AOD minimum in July [27] has disappeared in this study for the monthly evolution, thus indicating larger aerosol loads in the last summers. The progressive increase in AOD until summer is not observed in this case due to a lower mean value in March than in February. This could be caused by the occurrence of very intense dust episodes in February in the analyzed period, such as the one that took place from the 20 to 23 February 2017, reported by Fernández et al. [28], which masks the typical increase in AOD shown by the mentioned previous studies.

The AOD_{440} standard deviation values at night-time are larger than during the daytime for some months like March and October, which must be caused by some outliers, as pointed out by the P95 in these cases. These outliers may be AOD values contaminated by the presence of high and wispy ice clouds, like cirri. During the daytime, photometers measure the radiance on the sun's aureole in order to detect these thin clouds and classify those measurements as cloud-contaminated [21]; however, lunar aureole measurements are not carried out and, as a result, it is possible that occasionally AOD values measured under the presence of thin ice cloud pass the cloud-screening algorithm.

The results also show a good agreement between the values of the AOD_{440} interquartile range (IQR), which is the difference between Q3 and Q1, for sun- and moon-based measurements, thus indicating that dispersion of daytime and night-time AOD data is similar. In addition, P95 for AOD values present two peaks in March and August (around 0.37 for both day and night-time); on the other hand, the lowest P95 values occur in November, with 0.15 for daytime and 0.14 for night-time. For P5, the lowest values are found in January, with 0.032 for daytime, and in March, with 0.033 for night-time. The AODs at 380, 500, 675, 870, 1020 and 1640 nm show a similar behavior to the one described here for 440 nm, as can be seen in Figure A3 of the Appendix A.

Regarding the Ångström exponent (see Figure 2b), the mean and median are above 1.0 and below 1.5 for all months, showing no clear seasonal dependence and with slightly larger values during summer months. The AE values in summer indicate the continuous predominance of intermediate-sized particles at Valladolid, likely based on a mixture of clean continental aerosols [27], moderated African dust events and also, relatively frequently, polluted air masses from Europe. In addition, the maximum mean AE value occurs in July (mean value of about 1.42 for daytime and 1.35 for night-time). This could be caused by the presence of smoke from bushfires in the atmosphere, since this kind of aerosol corresponds to fine particles (i.e., very high AE values). Hence, the observed highest AOD_{440} values in summer months occur simultaneously with the largest AE values,

corroborating the impact of biomass burning events. The mean AE presents lower values for February and March (with a mean value for February of 1.12 during daytime and 1.13 for night-time, and for March, 1.08 during daytime and 1.15 for night-time); this coincides with some extreme Saharan desert dust episodes that occurred in these months at the Iberian Peninsula, as previously mentioned. The mean value for night-time in December is also very low, but differs from the value for daytime measurements. It can be seen that mean values remain smaller than median values for all months, possibly due to the low values of AE related to occasional Saharan dust transport events. There are similar mean values for AE during January and August, around 1.33, for both daytime and night-time measurements; but median daytime values remain smaller for August (around 1.35) than for January (around 1.46), with a larger difference between mean and median values. October and November have very similar median values. In general, the median AE values are similar during the daytime and night-time, when the median values are generally a little bit higher, except in December, when the night-time value is the lowest, showing an AE difference of about 0.2 from night-time to daytime. Perrone et al. [26] also found median values of AE to be higher at night-time except in winter season in Lecce. Pérez-Ramírez et al. [29] also observed these higher AE values at night-time, which were also more likely to be found in summer; these authors proposed that this is because for those months, convective activity is more intense during the daytime than at night-time, which can favor larger particles' deposition and an increase in AE values.

There are not large differences between the AE standard deviation values in March and October as it could be seen for AOD_{440}, but the standard deviation is generally higher for night-time than for daytime. The P95 values do not vary significantly but the P5 values seem to have a minimum value in spring months (0.23 for night-time in March), which is also related with the presence of extreme desert dust episodes, and then P5 of AE values increases for summer and autumn months (0.93 for daytime in September). The IQR values are lower for summer months, especially at night-time.

When the obtained AE values are compared with the AERONET $AE_{440\text{-}870}$ data of previous studies [22,27], mean values of both AE series are similar, except for the summer months, when the AE values are higher for the latest years. This result could be an indicator of an increase in the fine particles' presence in summer at Valladolid, likely caused by a higher occurrence of bushfires in the region.

Finally, the amount of daily daytime data is approximately twice the amount of night-time data, as can be seen in Figure 2c. This is because night-time measurements are only available for half of a whole moon cycle, as mentioned above (from the first to the third moon quarters). The lack of lunar data between the third and first moon quarters discussed above could explain some of the slight differences that have been observed between daytime and night-time values. The month with less data availability is April, which is linked with conditions of rain and cloud coverage in Valladolid that prevent the photometer from measuring frequently. The amount of night-time data is higher in the first months of the year because of longer nights in this period.

3.3. Daily Cycle

To study the pattern of the evolution of AOD_{440} and AE throughout the day, the hourly mean values of AOD and AE have been evaluated for each month using the same methodology as that used to find the daily mean values in the previous section. For a seasonal analysis of this pattern, Figure 3 presents the statistical estimators of hourly AOD_{440} and AE for one month of each season: January, April, July and October. Monthly analysis was selected instead of seasonal analysis to avoid the overlap of night-time and daytime data in the same hour. Even so, overlap occasionally occurs due to the change in the time of sunrise/sunset throughout a month. For those cases, both datasets have been used to compute the mean and the other statistical estimators. The months selected as representative for each season have no overlap or the overlap is minimal (October has

1 lunar observation and 25 solar observations at 17:00 UTC), but that is not the case for all months of the year.

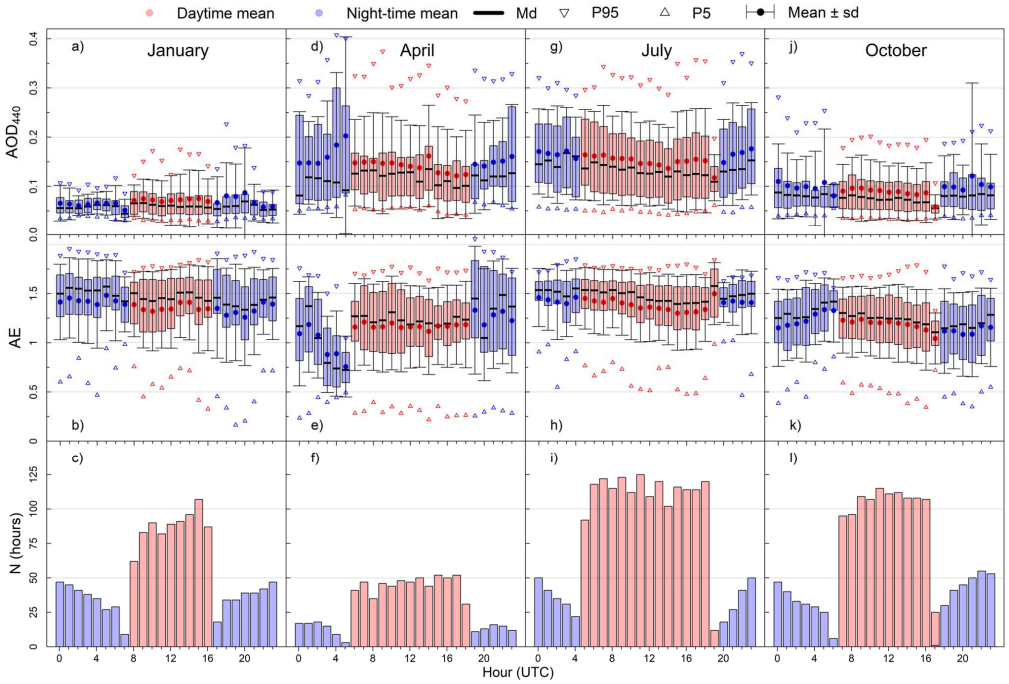

Figure 3. Distribution of daytime and night-time hourly aerosol optical depth at 440 nm (AOD_{440}) and Ångström exponent from 440 to 870 nm (AE) for January, April, July and October (**a**–**l**). The first (Q1) and third (Q3) quartile for the monthly dataset correspond to the upper and lower box limits. The median (Md) is represented by a horizontal black line, while the mean (M) is represented by a circle. The triangles show the 5th (P5) and 95th (P95) percentile values. The ± standard deviation is represented by an error bar centered on the mean value. The number of observations (N hours in each month) is shown in a histogram (panel (**d**)). Red values mean daytime, while blue is for night-time.

The mean and median of the AOD_{440} values shown in Figure 3 present good continuity between daytime and night-time for all months except close to sunrise and sunset. Those are the hours with the lowest amount of available night-time data; hence, the result could not be representative. The mean values of AOD_{440} are higher than the median values for all months, which must be caused by the presence of some high outliers, as the P95 value indicates. In July, the mean and median AOD_{440} values are higher during the first hours of the night (from 00:00 UTC), and then they decrease, being the median AOD_{440} value at 05:00 UTC equal to 0.16, higher than 0.12 reached at 19:00 UTC. In general, for the four months, the mean and median of the daytime AOD_{440} is higher early in the morning than at the end of the afternoon, showing a decreasing trend in AOD throughout the daytime, which is more appreciable in July.

The Q3 values of AOD_{440} in January are below 0.1, increasing during spring, as is observed for the month of April. The highest values appear during summer, as July shows, where the Q3 values are close to 0.2. Then, the Q3 values decrease during autumn, as can be seen in October. The IQRs in AOD_{440} values are similar between daytime and night-time for all months except in April. The standard deviation for AOD_{440} values is similar between daytime and night-time for each month. The P5 values of AOD_{440} do not present significant fluctuations throughout the day at any month, while the P95 values fluctuate but without a clear pattern. On the other hand, the Q1 and the P5 values of AOD_{440} are quite similar for all months, demonstrating that the seasonal differences are only reflected in the upper part of the data distribution.

Regarding AE, the mean and median values during the daytime and the night-time show good continuity for all months except in April at the end of the night; this is the only case in which the AE mean values are above median and both statistical estimators are below 1.0. In January, the median values are around 1.5, being even higher between 01:00 and 05:00 UTC. There are lower values in April than in January, possibly due to the presence of larger-sized particles like dust aerosols in spring. Although April displays a local minimum in terms of desert dust occurrence in the study region [24], desert dust event days in April are still more frequent than in January. For July, the mean AE value is very close to the median during daytime. In this month, there is a good correlation between day and night-time P95 values for AE, except for the values close to the sunrise and sunset, but this is unlikely to be representative since there is a small amount of data available for these hours.

For a more global analysis of the hourly data evolution in Valladolid, the same estimators of Figure 3 are presented in Figure 4, but they have been calculated considering all the available data together, giving an idea of a typical day of aerosol evolution in Valladolid. For certain hours, there is an overlap of night-time and daytime data due to the seasonal variation in the sunshine duration at mid latitudes.

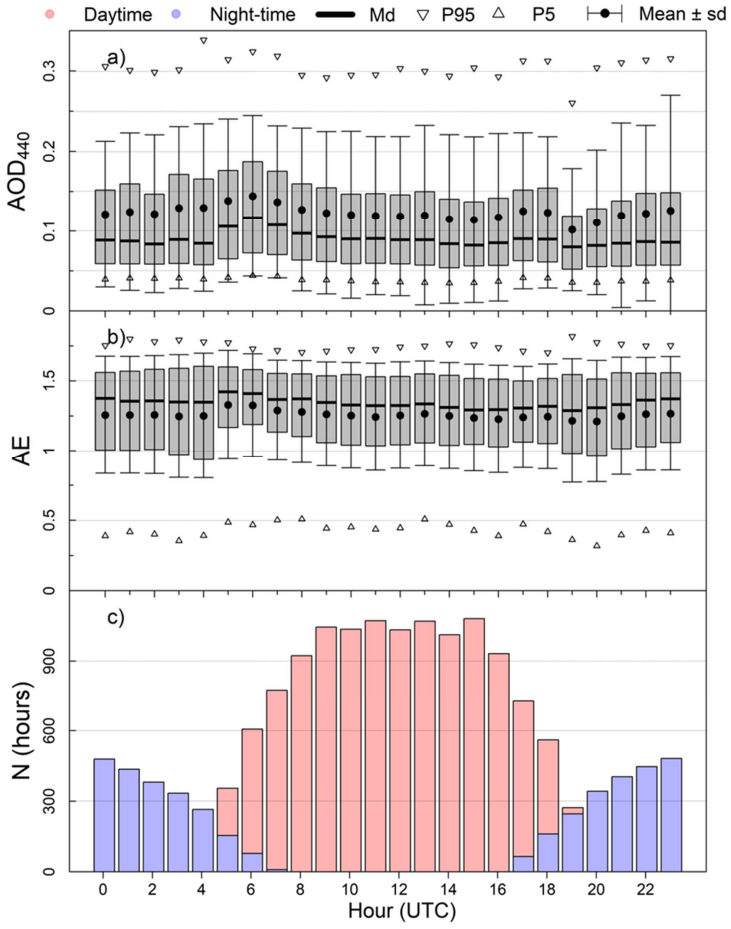

Figure 4. Distribution of daytime and night-time hourly aerosol optical depth at 440 nm (AOD_{440}; panel (**a**)) and Ångström exponent from 440 to 870 nm (AE; panel (**b**)) considering all available data (no distinction of month is made). The first (Q1) and third (Q3) quartile for the monthly dataset correspond to the upper and lower box limits. The median (Md) is represented by a horizontal black line, while the mean (M) is represented by a circle. The triangles show the 5th (P5) and 95th (P95) percentile values. The ± standard deviation is represented by an error bar centered on the mean value. The number of observations (N hours) is shown in a histogram (panel (**c**)). Red values mean daytime, while blue is for night-time.

The AOD_{440} data present a stable and continuous hourly evolution, with all the hourly mean and median values of AOD_{440} around 0.12 and 0.09, respectively. However, a pattern can be observed: the highest median AOD value appears close to sunrise (06:00 UTC), with a value of 0.12, and it slightly decreases until sunset (19:00 UTC), reaching the minimum median value of 0.07, when the median begins to increase until sunrise. A similar pattern occurs for the mean values of AOD_{440}, oscillating from 0.10 to 0.14, and for P95 values. The mentioned maximum values of AOD_{440} occurs when the hourly mean and median of AE are the highest (1.41 and 1.33, respectively), while the minimum mean value of AOD_{440} occurs for the lowest median AE value (1.21). This could be related to having stable atmospheric conditions that may prevent elimination processes, especially for fine particles. Analyzing the evolution of all the months in the year, it was found that for some months, the maximum AOD_{440} value is at 05:00 UTC, but the presence of some high values in March at 06:00 UTC, possibly caused by an intense dust transport event or cloud contamination, affect the mean value for all the time series. Regarding the AE, a similar pattern to that mentioned for AOD_{440} is also observed. The mean and median values are around 1.26 and 1.32, and the IQR is, in general, between 0.93 and 1.60. These IQRs and the standard deviation values are higher for night-time periods.

4. Summary and Conclusions

In this work, we have analyzed the seasonal and diurnal behavior of aerosol optical depth (AOD) and the Ångström exponent (AE) in Valladolid, Spain. The used data were obtained during the daytime and night-time with various sun–sky–lunar AERONET reference photometers between the years 2016 and 2022.

The results obtained show that there is an annual cycle, with maximum values of AOD during July and August and minimum values during January and December. There is a local minimum in May, which was also shown in previous studies in the same region. The lower AE values are seen from February to April; in summer, the values increase and remain stable until the end of the year. It is possible to see the transport of aerosol from biomass burning during summer, as the mean Ångström exponent (AE) values are not as low as expected for this season, when, typically, more but less-intense desert dust transport events occur.

In general, the same hourly patterns are observed throughout the seasons. Overall, results show that despite the different number of night-time and daytime observations, there is continuity between the statistical parameters provided by each type of data. Slightly higher median values were found for night-time measurements, particularly during summer months; this could be related to daily convective processes. Also, sky radiance measurements over the sun aureole are available during the daytime, and are useful for the cloud-screening of high and optically thin clouds, like cirri; however, these measurements are not available at night-time for lunar aureole, so some outliers during the night-time are likely contaminated by the presence of such high clouds. The AOD and AE values remain almost constant throughout the day except at sunrise and sunset, when there is less data availability. When computing the typical daily pattern of the entire dataset, the highest AOD value is found at 6:00 UTC and the lowest at 18:00 UTC.

To conclude, this study provides a better characterization of Valladolid's atmosphere. The results suggest that night-time data have good continuity with daytime data, and are necessary in order to complete the aerosol climatology, particularly at high-latitude sites, and to understand aerosol dynamics between day and night. A deeper study into the daily patterns could help to understand the smaller variations between sunrise and sunset. Also, improvements in the cloud-screening algorithms could help to reduce the uncertainties in these hours.

For future research, it would be advantageous to compare these patterns across various sites that also have sun–sky–moon photometers. Moreover, the availability of this kind of high-quality data enables the creation of a complete dataset for comparison and validation with measurements from other instruments that operate continuously, such as in situ

instrumentation or satellites. This dataset can also be implemented in conjunction with data from other instruments, including all-sky cameras, ceilometers, and lidars, which provide continuous measurements, in the retrieval of aerosols properties, to gain a deeper understanding of their behavior in the atmosphere.

Author Contributions: Conceptualization, C.H.d.B., D.M. and R.R.; methodology, D.M. and R.R.; software, R.G.; validation, C.H.d.B., D.M., R.R., R.G., S.H.-A., D.G.-F., A.C., C.T., V.E.C. and Á.M.D.F.B.; formal analysis, C.H.d.B., D.M. and R.R.; investigation, C.H.d.B., D.M. and R.R.; resources, C.H.d.B., D.M., R.R., R.G., S.H.-A., D.G.-F., A.C., C.T., V.E.C. and Á.M.D.F.B.; data curation, R.R.; writing—original draft preparation, C.H.d.B., D.M. and R.R.; writing—review and editing, C.H.d.B., D.M., R.R., R.G., S.H.-A., D.G.-F., A.C., C.T., V.E.C. and Á.M.D.F.B.; visualization, C.H.d.B., D.M. and R.R.; supervision, R.R., C.T., V.E.C. and Á.M.D.F.B.; project administration, R.R., C.T., V.E.C. and Á.M.D.F.B.; funding acquisition, R.R., C.T., V.E.C. and Á.M.D.F.B. All authors have read and agreed to the published version of the manuscript.

Funding: This research has been supported by the Ministerio de Ciencia e Innovación (grant no. PID2021-127588OB-I00), the Junta de Castilla y León (grant no. VA227P20) and EMPIR within the joint research project 19ENV04 MAPP. This publication is part of the TED2021-131211B-I00 project funded by MCIN/AEI/10.13039/501100011033 and European Union "NextGenerationEU"/PRTR. This article is based on work from COST Action CA21119 HARMONIA, supported by COST (European Cooperation in Science and Technology).

Data Availability Statement: The photometers from AERONET's site at Valladolid were used for obtaining the metadata. Aerosol Optical Depth and Ångstrom exponent products were obtained with the CÆLIS tool (www.caelis.uva.es, accessed on 8 November 2023) (Gonzalez, 2020). These products are available on request.

Acknowledgments: The authors thank the GOA-UVa staff members Rogelio Carracedo, Patricia Martín-Sánchez, Javier Gatón and José Luis Martín who helped with the maintenance of the instruments and support for the station infrastructure.

Conflicts of Interest: The authors declare no conflict of interest.

Appendix A

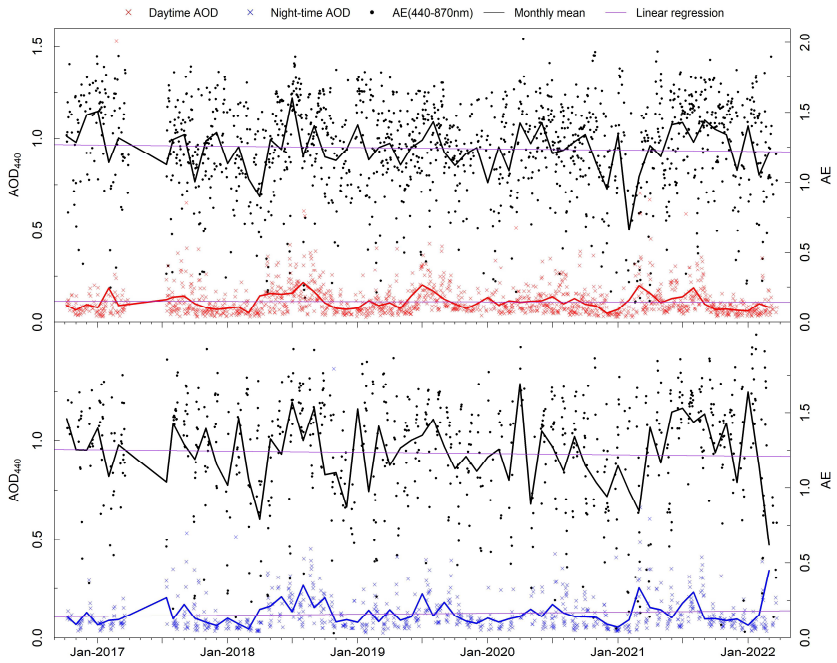

Figure A1. Daily mean for nocturnal measurements of AOD at 440 nm (AOD_{440}) and AE in Valladolid. Solid lines are the monthly mean values. Red color is used for daytime measurements and blue for night-time.

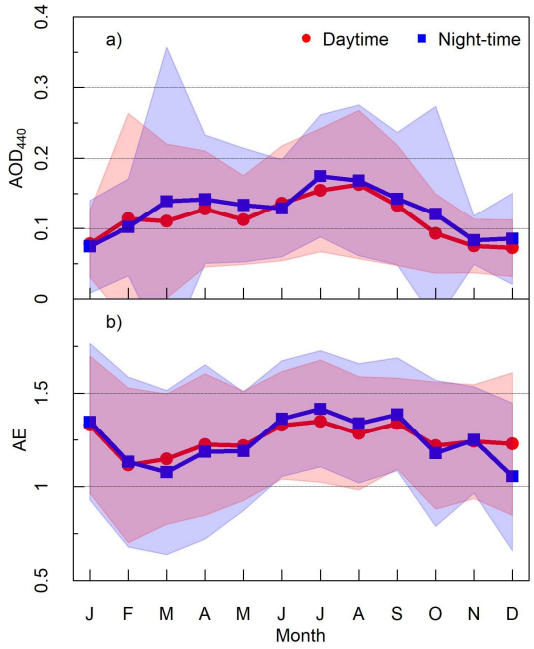

Figure A2. Monthly means for diurnal and nocturnal measurements of aerosol optical depth at 440 nm (AOD_{440}) (**a**) and Ångström exponent from 440 to 870 nm (AE) (**b**) in Valladolid. Solid lines are the monthly mean values; the ± standard deviation centered on the mean value is represented by the colored regions. Red color is used for daytime measurements and blue for night-time.

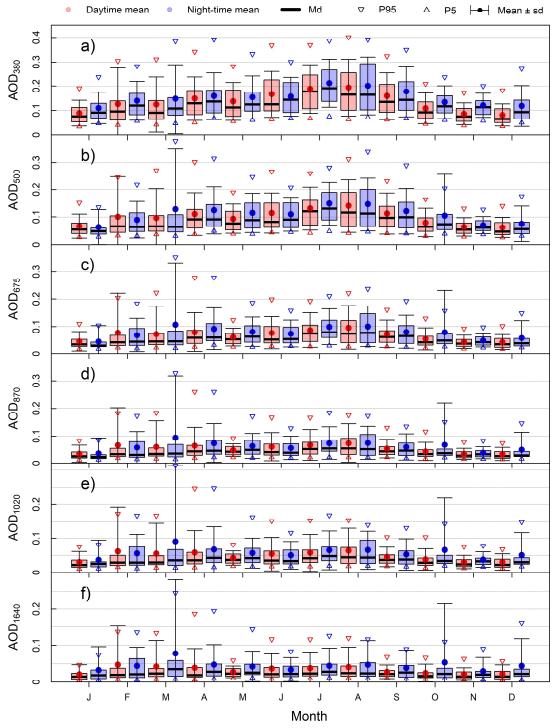

Figure A3. Box plot for the monthly evolution of AOD at 380 nm (AOD_{380}; panel (**a**)), 500 nm (AOD_{500}; panel (**b**)), 675 nm (AOD_{675}; panel (**c**)), 870 nm (AOD_{870}; panel (**d**)), 1020 nm (AOD_{1020}; panel (**e**)) and 1640 nm (AOD_{1640}; panel (**f**)) at Valladolid. The first (Q1) and third (Q3) quartile for the monthly dataset correspond to the upper and lower box limits. The median (Md) is represented by a horizontal black line, while the mean (M) is represented by a circle. The triangles show the 5th (P5) and 95th (P95) percentile values. The ± standard deviation is represented by an error bar centered on the mean value.

References

1. Boucher, O.; Randall, D.; Artaxo, P.; Bretherton, C.; Feingold, G.; Forster, P.; Kerminen, V.; Kondo, Y.; Liao, H.; Lohmann, U.; et al. Clouds and Aerosols. In *Climate Change 2013: The Physical Science Basis. Contribution of Working Group I to the Fifth Assessment Report of the Intergovernmental Panel on Climate Change Coordinating Lead Authors: Lead Authors*; Cambridge University Press: Cambridge, UK, 2013.
2. Shindell, D.; Faluvegi, G.; Nazarenko, L.; Bowman, K.; Lamarque, J.F.; Voulgarakis, A.; Schmidt, G.A.; Pechony, O.; Ruedy, R. Attribution of Historical Ozone Forcing to Anthropogenic Emissions. *Nat. Clim. Chang.* **2013**, *3*, 567–570. [CrossRef]
3. Szopa, S.; Naik, V.; Adhikary, B.; Artaxo, P.; Berntsen, T.; Collins, W.; Fuzzi, S.; Gallardo, L.; Kiendler-Scharr, A.; Klimont, Z.; et al. Short-Lived Climate Forcers. In *Climate Change 2021: The Physical Science Basis. Contribution of Working Group I to the Sixth Assessment Report of the Intergovernmental Panel on Climate Change*; Masson-Delmotte, V., Zhai, P., Pirani, A., Connors, S.L., Péan, C., Berger, S., Caud, N., Chen, Y., Goldfarb, L., Gomis, M.I., et al., Eds.; Cambridge University Press: Cambridge, UK, 2021; pp. 817–922.
4. Ångström, A. Techniques of Determinig the Turbidity of the Atmosphere. *Tellus* **1961**, *13*, 214–223. [CrossRef]
5. Cachorro, V.E.; Casanova, J.L.; de Frutos, A.M. The Influence of Ångström Parameters on Calculated Direct Solar Spectral Irradiances at High Turbidity. *Sol. Energy* **1987**, *39*, 399–407. [CrossRef]
6. Holben, B.N.; Eck, T.F.; Slutsker, I.; Tanré, D.; Buis, J.P.; Setzer, A.; Vermote, E.; Reagan, J.A.; Kaufman, Y.J.; Nakajima, T.; et al. AERONET—A Federated Instrument Network and Data Archive for Aerosol Characterization. *Remote Sens. Environ.* **1998**, *66*, 1–16. [CrossRef]
7. Wehrli, C. GAWPFR: A Network of Aerosol Optical Depth Observations with Precision Filter Radiometers. In Proceedings of the WMO/GAW Experts Workshop on a Global Surface Based Network for Long Term Observations of Column Aerosol Optical Properties, Davos, Switzerland, 8–10 March 2004.
8. Nakajima, T.; Campanelli, M.; Che, H.; Estellés, V.; Irie, H.; Kim, S.-W.; Kim, J.; Liu, D.; Nishizawa, T.; Pandithurai, G.; et al. An Overview of and Issues with Sky Radiometer Technology and SKYNET. *Atmos. Meas. Tech.* **2020**, *13*, 4195–4218. [CrossRef]
9. Barreto, Á.; Cuevas, E.; Granados-Muñoz, M.-J.; Alados-Arboledas, L.; Romero, P.M.; Gröbner, J.; Kouremeti, N.; Almansa, A.F.; Stone, T.; Toledano, C.; et al. The New Sun-Sky-Lunar Cimel CE318-T Multiband Photometer—A Comprehensive Performance Evaluation. *Atmos. Meas. Tech.* **2016**, *9*, 631–654. [CrossRef]
10. Barreto, A.; Cuevas, E.; Damiri, B.; Romero, P.M.; Almansa, F. Column Water Vapor Determination in Night Period with a Lunar Photometer Prototype. *Atmos. Meas. Tech.* **2013**, *6*, 2159–2167. [CrossRef]
11. Kieffer, H.H.; Stone, T.C. The Spectral Irradiance of the Moon. *Astron. J.* **2005**, *129*, 2887–2901. [CrossRef]
12. Barreto, A.; Román, R.; Cuevas, E.; Pérez-Ramírez, D.; Berjón, A.J.; Kouremeti, N.; Kazadzis, S.; Gröbner, J.; Mazzola, M.; Toledano, C.; et al. Evaluation of Night-Time Aerosols Measurements and Lunar Irradiance Models in the Frame of the First Multi-Instrument Nocturnal Intercomparison Campaign. *Atmos. Environ.* **2019**, *202*, 190–211. [CrossRef]
13. Barreto, Á.; Román, R.; Cuevas, E.; Berjón, A.J.; Almansa, A.F.; Toledano, C.; González, R.; Hernández, Y.; Blarel, L.; Goloub, P.; et al. Assessment of Nocturnal Aerosol Optical Depth from Lunar Photometry at the Izaña High Mountain Observatory. *Atmos. Meas. Tech.* **2017**, *10*, 3007–3019. [CrossRef]
14. Román, R.; González, R.; Toledano, C.; Barreto, Á.; Pérez-Ramírez, D.; Benavent-Oltra, J.A.; Olmo, F.J.; Cachorro, V.E.; Alados-Arboledas, L.; de Frutos, A.M.; et al. Correction of a Lunar-Irradiance Model for Aerosol Optical Depth Retrieval and Comparison with a Star Photometer. *Atmos. Meas. Tech.* **2020**, *13*, 6293–6310. [CrossRef]
15. Fuertes, D.; Toledano, C.; González, R.; Berjón, A.; Torres, B.; Cachorro, V.E.; De Frutos, Á.M. CÆLIS: Software for Assimilation, Management and Processing Data of an Atmospheric Measurement Network. *Geosci. Instrum. Methods Data Syst.* **2018**, *7*, 67–81. [CrossRef]
16. González, R.; Toledano, C.; Román, R.; Fuertes, D.; Berjón, A.; Mateos, D.; Guirado-Fuentes, C.; Velasco-Merino, C.; Antuña-Sánchez, J.C.; Calle, A.; et al. Daytime and Nighttime Aerosol Optical Depth Implementation in CÆLIS. *Geosci. Instrum. Methods Data Syst.* **2020**, *9*, 417–433. [CrossRef]
17. Kouremeti, N.; Gröbner, J.; Kazadzis, S.; Pfiffner, D.; Soder, R. *Development of a Lunar PFR PMOD/WRC Annual Report 2015 Eth-22636-17_2015*; ETH Zurich: Zürich, Switzerland, 2016.
18. Uchiyama, A.; Shiobara, M.; Kobayashi, H.; Matsunaga, T.; Yamazaki, A.; Inei, K.; Kawai, K.; Watanabe, Y. Nocturnal Aerosol Optical Depth Measurements with Modified Sky Radiometer POM-02 Using the Moon as a Light Source. *Atmos. Meas. Tech.* **2019**, *12*, 6465–6488. [CrossRef]
19. Bennouna, Y.S.; Cachorro, V.E.; Mateos, D.; Burgos, M.A.; Toledano, C.; Torres, B.; de Frutos, A.M. Long-Term Comparative Study of Columnar and Surface Mass Concentration Aerosol Properties in a Background Environment. *Atmos. Environ.* **2016**, *140*, 261–272. [CrossRef]
20. Toledano, C.; González, R.; Fuertes, D.; Cuevas, E.; Eck, T.F.; Kazadzis, S.; Kouremeti, N.; Gröbner, J.; Goloub, P.; Blarel, L.; et al. Assessment of Sun Photometer Langley Calibration at the High-Elevation Sites Mauna Loa and Izaña. *Atmos. Chem. Phys.* **2018**, *18*, 14555–14567. [CrossRef]
21. Giles, D.M.; Sinyuk, A.; Sorokin, M.G.; Schafer, J.S.; Smirnov, A.; Slutsker, I.; Eck, T.F.; Holben, B.N.; Lewis, J.R.; Campbell, J.R.; et al. Advancements in the Aerosol Robotic Network (AERONET) Version 3 Database—Automated near-Real-Time Quality Control Algorithm with Improved Cloud Screening for Sun Photometer Aerosol Optical Depth (AOD) Measurements. *Atmos. Meas. Tech.* **2019**, *12*, 169–209. [CrossRef]

22. Mateos, D.; Cachorro, V.E.; Toledano, C.; Burgos, M.A.; Bennouna, Y.; Torres, B.; Fuertes, D.; González, R.; Guirado, C.; Calle, A.; et al. Columnar and Surface Aerosol Load over the Iberian Peninsula Establishing Annual Cycles, Trends, and Relationships in Five Geographical Sectors. *Sci. Total Environ.* **2015**, *518–519*, 378–392. [CrossRef] [PubMed]
23. López-Cayuela, M.Á.; Córdoba-Jabonero, C.; Bermejo-Pantaleón, D.; Sicard, M.; Salgueiro, V.; Molero, F.; Carvajal-Pérez, C.V.; Granados-Muñoz, M.J.; Comerón, A.; Couto, F.T.; et al. Vertical Characterization of Fine and Coarse Dust Particles during an Intense Saharan Dust Outbreak over the Iberian Peninsula in Springtime 2021. *Atmos. Chem. Phys.* **2023**, *23*, 143–161. [CrossRef]
24. Cachorro, V.E.; Burgos, M.A.; Mateos, D.; Toledano, C.; Bennouna, Y.; Torres, B.; De Frutos, Á.M.; Herguedas, Á. Inventory of African Desert Dust Events in the North-Central Iberian Peninsula in 2003–2014 Based on Sun-Photometer–AERONET and Particulate-Mass–EMEP Data. *Atmos. Chem. Phys.* **2016**, *16*, 8227–8248. [CrossRef]
25. Mateos, D.; Cachorro, V.E.; Velasco-Merino, C.; O'Neill, N.T.; Burgos, M.A.; Gonzalez, R.; Toledano, C.; Herreras, M.; Calle, A.; de Frutos, A.M. Comparison of Three Different Methodologies for the Identification of High Atmospheric Turbidity Episodes. *Atmos. Res.* **2020**, *237*, 104835. [CrossRef]
26. Perrone, M.R.; Lorusso, A.; Romano, S. Diurnal and Nocturnal Aerosol Properties by AERONET Sun-Sky-Lunar Photometer Measurements along Four Years. *Atmos. Res.* **2022**, *265*, 105889. [CrossRef]
27. Mateos, D.; Antón, M.; Toledano, C.; Cachorro, V.E.; Alados-Arboledas, L.; Sorribas, M.; Costa, M.J.; Baldasano, J.M. Aerosol Radiative Effects in the Ultraviolet, Visible, and near-Infrared Spectral Ranges Using Long-Term Aerosol Data Series over the Iberian Peninsula. *Atmos. Chem. Phys.* **2014**, *14*, 13497–13514. [CrossRef]
28. Fernández, A.J.; Sicard, M.; Costa, M.J.; Guerrero-Rascado, J.L.; Gómez-Amo, J.L.; Molero, F.; Barragán, R.; Basart, S.; Bortoli, D.; Bedoya-Velásquez, A.E.; et al. Extreme, Wintertime Saharan Dust Intrusion in the Iberian Peninsula: Lidar Monitoring and Evaluation of Dust Forecast Models during the February 2017 Event. *Atmos. Res.* **2019**, *228*, 223–241. [CrossRef]
29. Pérez-Ramírez, D.; Lyamani, H.; Olmo, F.J.; Alados-Arboledas, L. Improvements in Star Photometry for Aerosol Characterizations. *J. Aerosol Sci.* **2011**, *42*, 737–745. [CrossRef]